

Proton CT

A novel diagnostic tool in cancer therapy

Monika Varga-Kofarago

MTA Wigner RCP

on behalf of the pCT Collaboration

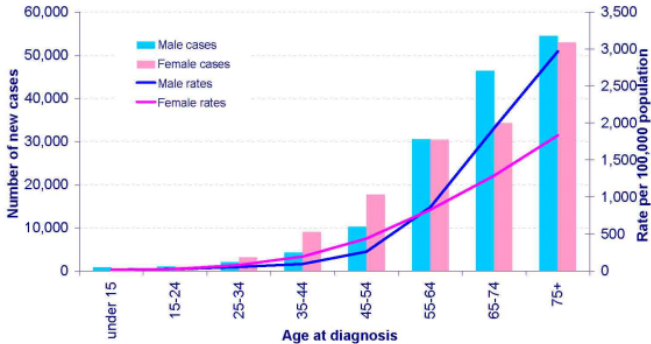
7th December 2018

Zimányi School

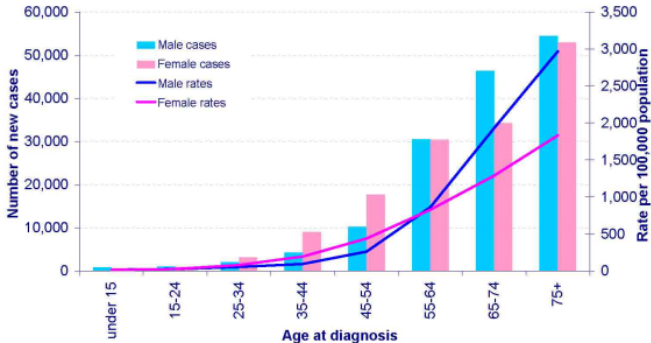


This work has been supported by the Hungarian NKFIH/OTKA K 120660 grant.

Cancer statistics and therapies



Cancer statistics and therapies



- Contributions to successful treatment of cancer
 - 45-50% surgery
 - 40-50% radiotherapy
 - 10-15% chemotherapy
- Radiotherapy is an important weapon in the battle against cancer

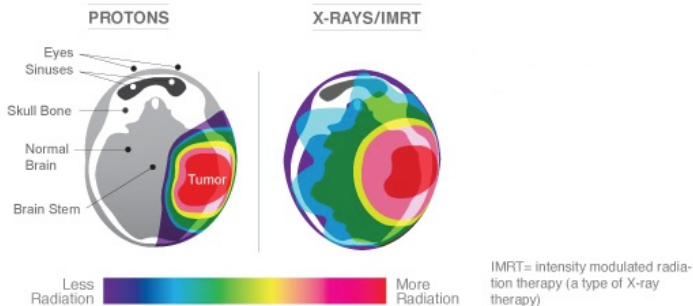
K. Peach, Heavy Ions in Science and Health workshop, Bergen, 2012

Radiotherapy and its problems

- Goal: damage the DNA of cancer cells
- Direct or indirect ionization
- Treatment with photons or charged particles (e.g. protons)
- Photons: mostly indirect ionization through forming free radicals
- Protons: mostly direct ionization

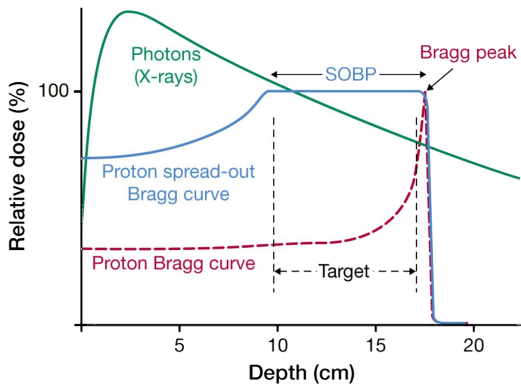
Radiotherapy and its problems

- Goal: damage the DNA of cancer cells
- Direct or indirect ionization
- Treatment with photons or charged particles (e.g. protons)
- Photons: mostly indirect ionization through forming free radicals
- Protons: mostly direct ionization
- Need to minimize the damage to healthy tissue



Source: ProCure Training and Development Center

Hadron therapy – advantages



R. Mohan, A. Mahajan and B. D. Minsky,
Clin Cancer Res December 1 2013 (19) (23)
6338-6343
DOI: 10.1158/1078-0432.CCR-13-0614

© 2013 American Association for Cancer Research

- **Photons** are absorbed mostly at the entrance
- **Charged particles**
 - lose most of their energy in the Bragg peak
 - Relatively low dose in front of the tumor
 - Sharp fall-off of dose deposition (<mm)

Particle therapy centres in Europe - 2015

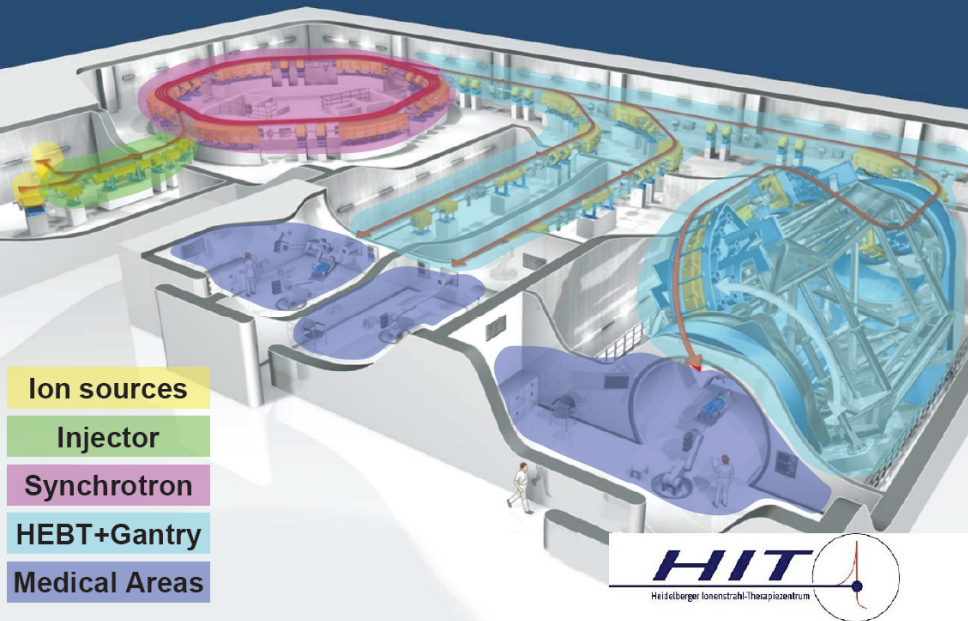


Source: PTCOG, October 2015

- 27 proton centers
- Three C-ion centers

M. Dosanjh, M. Cirilli, S. Myers, S. Navin (2016). Medical applications at CERN and the ENLIGHT network. *Frontiers in Oncology*. 6. 10.3389/fonc.2016.00009.

Treatment facilities

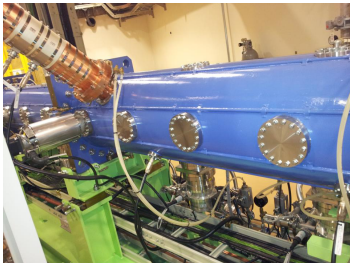


Treatment facilities

Ion source



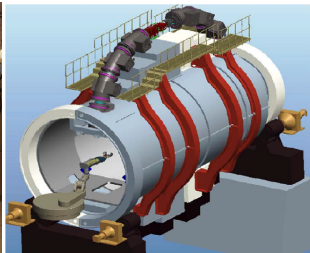
LINAC



Synchrotron



Treatment room



Superconducting gantry



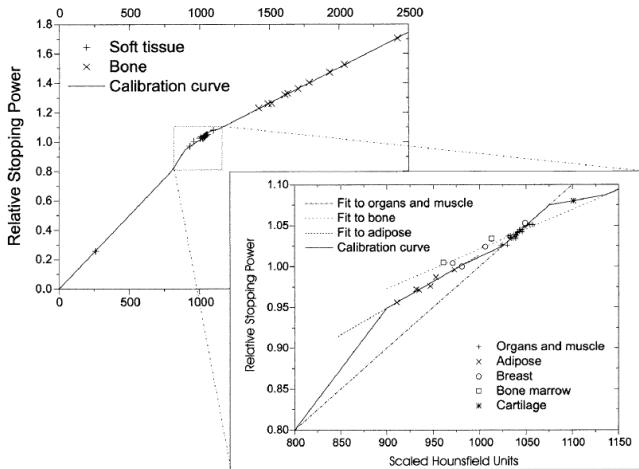
Extraction and beam transport

- Stopping power in front of the tumor to be known precisely
- Stopping power is described by Bethe-Bloch formula:

$$dE/dx \sim \text{electron density} \times \ln \frac{\text{max. energy transfer in single collision}}{\text{effective ionization potential}^2}$$

- Derive stopping power from X-ray CT
- X-ray attenuation in tissue depends also strongly on Z (Z^5 for photoelectric effect)

Proton therapy – missing information



- Scaled Hounsfield Units (scanner specific) \sim attenuation coefficient
- Not a clear relation with the stopping power

Schaffner, B. and E. Pedroni, Phys Med Biol, 1998. 43(6): p. 1579-92.

Range uncertainties and scattering

- Single energy CT: up to 7.4% uncertainty
- Target volume is increased by up to 1 cm in beam direction
- Avoid beam directions with a critical organ behind the tumor
- Dual energy CT: up to 1.7% uncertainty
- Proton CT: up to 0.3% uncertainty

A comparison of dual energy CT and proton CT for stopping power estimation

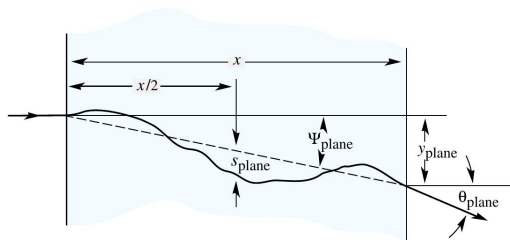
D. C. Hansen, J. Seco, T. S. Sorensenn, J. B. B. Petersen, J. E. Wildberger, F. Verhaegen and G. Landry

Range uncertainties and scattering

- Single energy CT: up to 7.4% uncertainty
- Target volume is increased by up to 1 cm in beam direction
- Avoid beam directions with a critical organ behind the tumor
- Dual energy CT: up to 1.7% uncertainty
- Proton CT: up to 0.3% uncertainty

A comparison of dual energy CT and proton CT for stopping power estimation

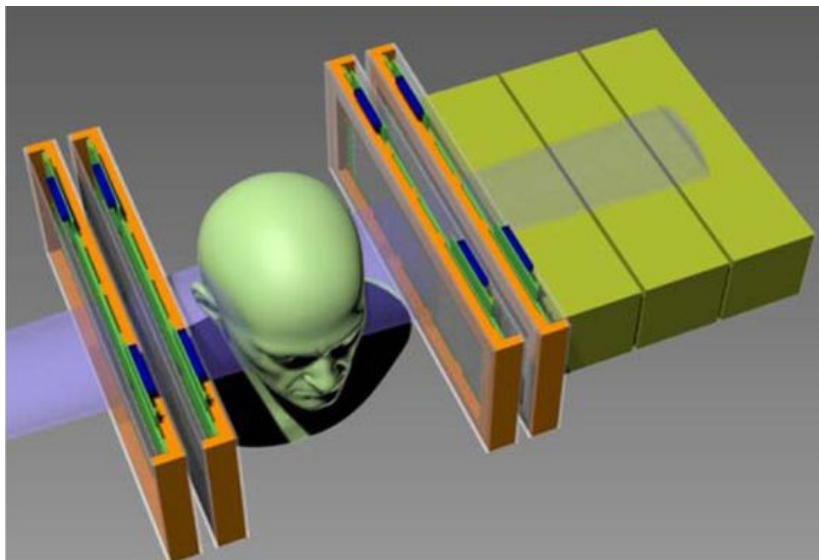
D. C. Hansen, J. Seco, T. S. Sorensenn, J. B. B. Petersen, J. E. Wildberger, F. Verhaegen and G. Landry



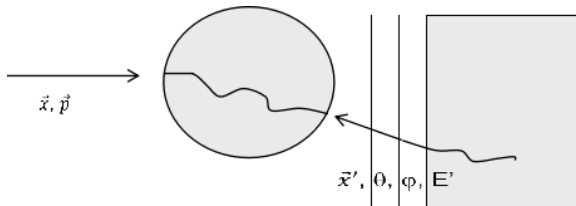
M. Tanabashi et al. (Particle Data Group), Phys. Rev. D 98, 030001 (2018)

- Multiple Coulomb scattering in the material
- Measurement before and after the patient needed

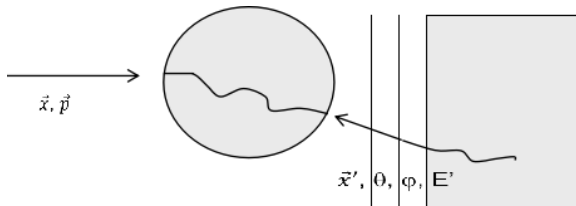
Proton CT – concept



H.F.-W. Sadrozinski, Nuclear Instruments and Methods in Physics Research A 732 (2013) 34-39



- \vec{x} and \vec{p} from beam optics and scanning system
- $\vec{x}', \theta, \varphi$ and E' to be measured
- Reconstruction of trajectories in 3D \rightarrow place of irradiation
- Measurement of range in external absorber \rightarrow lost energy



- \vec{x} and \vec{p} from beam optics and scanning system
- \vec{x}' , θ , φ and E' to be measured
- Reconstruction of trajectories in 3D \rightarrow place of irradiation
- Measurement of range in external absorber \rightarrow lost energy
- Before the treatment \rightarrow 3D map of electron density in target
- Quasi-simultaneously with therapeutic beam
 - Patient alignment
 - Online verification of dose
 - Dose optimization

Requirements of the detector

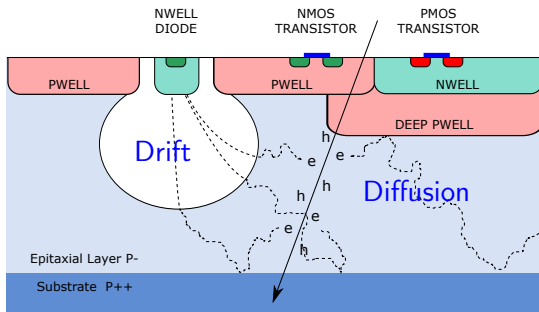
- High position resolution (tens of μm)
- Simultaneous tracking of large particle multiplicities ($10^7 - 10^9$ protons/s)
- Fast readout
- Radiation hardness
- Front detector: low mass, thin sensors (50 – 100 μm)
- Back detector: good range resolution



- High granularity digital sampling calorimeter
- Monolithic Active Pixel Sensors (MAPS) as active layers

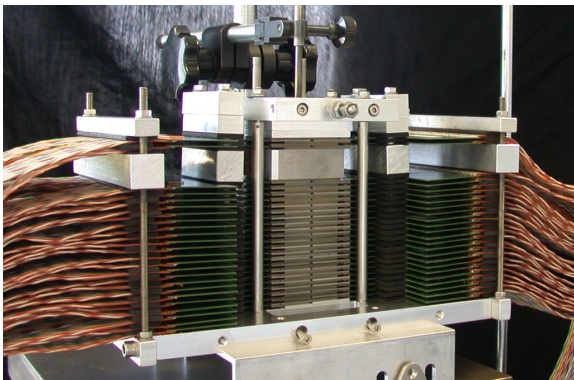
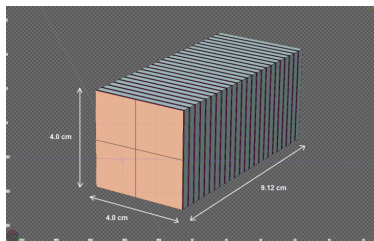
Monolithic Active Pixel Sensors (MAPS)

- Silicon sensors
- Using TowerJazz 0.18 μm CMOS imaging process
- High-resistivity ($> 1\text{k}\Omega\text{ cm}$) epitaxial layer on p-type substrate
- Deep PWELL shields NWELL of PMOS transistors
 - Allows full CMOS circuitry in active area
- Moderate reverse substrate biasing possible
 - Larger depletion volume



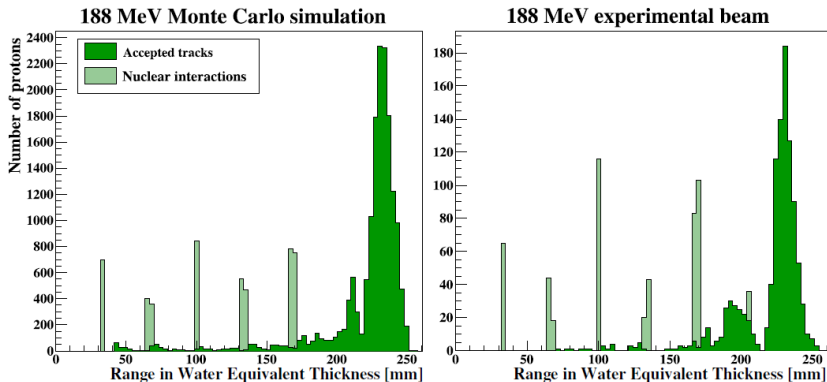
Digital calorimeter prototypes

- Silicon-tungsten sampling calorimeter (constructed at Utrecht University)
- Optimized for electromagnetic showers
- Active layers: MAPS (MIMOSA 23 – IPHC Strasbourg)
- Compact design $4 \times 4 \times 11.6 \text{ cm}^3$
- 24 layers
- Absorbers: 3.5 mm of W



NIMA 860, 51-61, 2017,
<https://arxiv.org/abs/1611.02031>
Jinst 13, P01014, 2018,
<https://arxiv.org/abs/1708.05164>

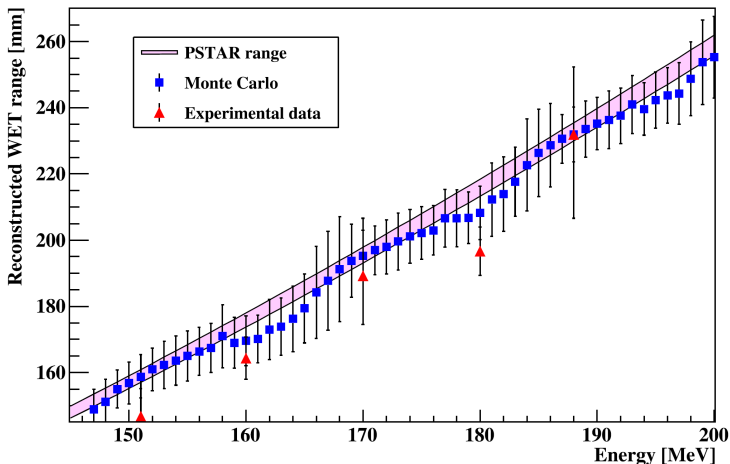
Results from the prototype



H. Pettersen, PhD thesis, UiB, 2018

- Data was taken at KVI in Groningen with 188 MeV protons
- Good agreement between data and simulations

Results from the prototype

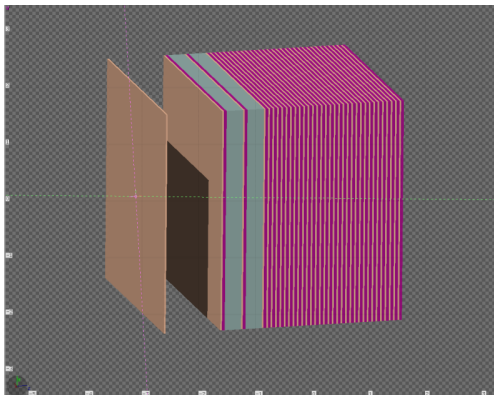


H. Pettersen, PhD thesis, UiB, 2018

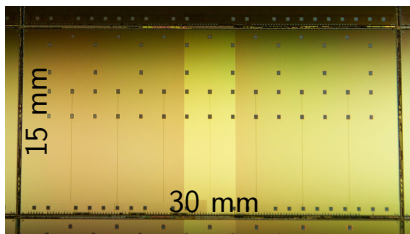
- Data was taken at KVI in Groningen
- Good agreement between data and simulations

Optimization of the design

- Absorber
 - Energy degrader, mechanical carrier, cooling medium
 - Material choice: Al
 - Thickness: 3.5 mm
- Longitudinal segmentation
 - Number of sensitive and absorber layers: 41
- Geometry
 - Front area: 27 cm x 15 cm

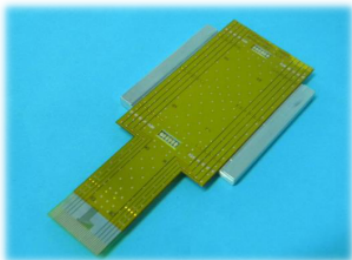


- ALPIDE – **ALICE** **PI**xel **DE**tector
- Developed for the upgrade of the ALICE Inner Tacker System
- Large silicon sensor (15 mm × 30 mm)
- 512 × 1024 pixels
- Pixels are 27 μm × 29 μm
- Digital readout with priority encoder
- Thin sensor (50 μm or 100 μm)
- Efficiency > 99%
- Resolution ~ 5 μm



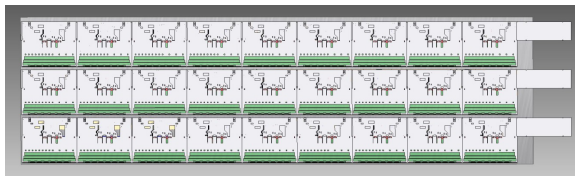
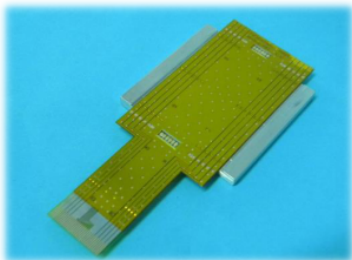
Mounting

- ALPIDE mounted on thin flex cables
 - Aluminum-polyamide dielectrics: 30 μm Al, 20 μm plastic
 - Design and production:
Utrecht University, Netherlands and LTU, Kharkiv, Ukraine
- Intermediate prototype
 - Chip cable with two ALPIDE sensors



Picture from LTU

- ALPIDE mounted on thin flex cables
 - Aluminum-polyamide dielectrics: 30 μm Al, 20 μm plastic
 - Design and production:
Utrecht University, Netherlands and LTU, Kharkiv, Ukraine
- Intermediate prototype
 - Chip cable with two ALPIDE sensors
- Final system
 - Flexible carrier board modules with 2×3 strings with 9 chips



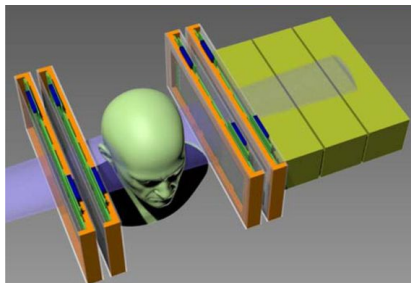
Picture from Utrecht University

Conclusions

- Hadron therapy → lower unnecessary dose for the patient
- Uncertainty in energy loss from extrapolation from CT
- pCT: powerful imaging tool to reduce the uncertainty
- Digital sampling calorimeter made of ALPIDE sensors
- First sensor module by the end of the year

Collaboration:

- University of Bergen
- Helse Bergen
- Utrecht University
- DKFZ Heidelberg
- Wigner Budapest
- Western Norway University of Applied Sciences



Thank you for your attention!

BACKUP